

Springer

This document is the Accepted Manuscript version of a Published Work that appeared in final form in Journal of Materials Science, copyright © Springer after peer review and technical editing by the publisher.

To access the final edited and published work see

<http://link.springer.com/article/10.1007/s10973-016-5392-z>.

IMPROVED FIRE RESISTANCE BY USING SLAG CEMENTS

Éva Lubl¹, Katalin Kopecsk², György L. Balázs¹, Imre Miklós Szilágyi^{3,4}, János Madarász³

¹Budapest University of Technology and Economics, Department of Construction Materials and Technologies, H-1521 Budapest, Hungary, lubeva@web.de, Phone: +36-20-3193876

²Budapest University of Technology and Economics, Department of Engineering Geology and Geotechnics, H-1521 Budapest, Hungary

³Budapest University of Technology and Economics, Department of Inorganic and Analytical Chemistry, Szent Gellért tér 4., Budapest, H-1111, Hungary;

⁴MTA-BME Technical Analytical Chemistry Research Group of the Hungarian Academy of Sciences, Szent Gellért tér 4., Budapest, H-1111, Hungary;

Abstract

Concrete is a composite material that mainly consists of mineral aggregates bound by matrix of hardened cement paste. Composition and microstructure of hardened cement paste have important influences on the properties of concrete exposed to high temperatures. An extensive experimental study was carried out to analyze the post-heating characteristics of concretes subjected to temperatures up to 800 °C. Major parameters of our study were the slag content of cement (0, 16, 25, 41 or 66 m%) and the value of maximum annealing temperature.

Our results indicated that (i) the number and size of surface cracks as well as compressive strength decreased by the increasing slag content of cements due to elevated temperature; (ii) the most intensive surface cracking was observed by using Portland cement without addition of slag.

The increasing slag content of cement increased relative post-heating compressive strength. Tendencies of surface cracking and reduction of compressive strength were in agreement, i.e. the more surface cracks, the more strength reduction.

Keywords: Temperature, Thermal analysis, Compressive strength, Ca(OH)₂, Fire

1. Introduction

Effects of high temperatures on the mechanical properties of concrete were studied as early as the 1940s [1]. In the 1960s and 1970s fire research was mainly directed to study the behaviour of concrete structural elements [2]. There was relatively few information on the concrete properties during and after fire [3].

Recent fire cases called again the attention to fire research. Different concrete types may also mean different possibilities for fire design [4-6]. Environmental protection requires the use of cements with low clinker content. Present study is directed to the influence of high temperatures on specimens made of cements with different slag contents. Concrete is a composite material that consists mainly of mineral aggregates bound by a matrix of hardened cement paste. Composition and internal structure of hardened cement paste has an important influence on the properties of concrete exposed to high temperatures [7]. Characteristics of concrete during and after the heating process depend on the type of cement, the type of aggregate and the interaction between them [8-10].

Effect of cement type has been hardly studied. Early studies on concretes made of the two commonly used cement types, Portland cement or Portland cement with low amount of slag indicated almost the same residual compressive strength over 400 °C [11, 12]. The properties of cement paste itself are also influenced by the mixing proportions of the constituents [13-15]. Behaviour at high temperatures depends on parameters like water/cement ratio, amount of CSH (calcium-silicate-hydrates), amount of Ca(OH)_2 and degree of hydration. Different cement pastes can perform differently in fire [16].

Grainger [17] studied cements with or without pulverised fly ash (PFA) subjected to a series of temperatures ranging from 100 °C to 600 °C with an interval of 100 °C. In his research the dosage of PFA was 20 %, 25 %, 37.5 % and 50 % of the total mass of binders. It was found that the addition of PFA could improve the residual compressive strength of cement paste. The beneficial effect of PFA as part of the binder was in good agreement with the results of Dias et al [18] and Xu et al [19]. Khoury et al observed that 400 °C was a critical temperature for Portland cement concretes, above which concretes would disintegrate on subsequent post cooling exposure to ambient conditions [20].

In fire, the heated surface region of concrete loses its moisture content by evaporation from the surface and by migration into the inner concrete mass driven by the temperature gradient [21, 22]. Due to high temperatures, structure and mineral content of concrete changes. The analysis was made by thermogravimetry (TG). Around 100 °C the mass-loss is caused by water evaporating from the micropores. The decomposition of ettringite

($3\text{CaOAl}_2\text{O}_3 \cdot 3\text{CaSO}_4 \cdot 32\text{H}_2\text{O}$) takes place between 50 °C and 110 °C. At 200 °C there is a further dehydration, which causes small mass loss. The mass loss of the test specimens with various moisture contents was different till all the pore water and chemically bound water were gone. Further mass loss was not perceptible around 250-300 °C [23, 24]. During heating the endothermic dehydration of $\text{Ca}(\text{OH})_2$ takes place between temperatures of 450 °C and 550 °C (1). This endothermic reaction is accompanied by loss of mass [25].



In the case of concretes made of quartz gravel aggregate, other influencing factor is the change in crystal structure of quartz α formation into β formation at 573 °C. This transformation followed by 5.7 % volumetric increase that influences the strength detrimentally [26]. Dehydration of calcium-silicate-hydrates was found at the temperature of 700 °C [27]. Based on these information, we carried out an extensive experimental study to analyze the post-heating characteristics of concretes subjected to temperatures up to 800 °C. Major parameter of our study was the slag content of cement (0, 16, 25, 41 or 66 m%) in addition to the value of maximum annealing temperature.

2. Experimental program

2.1 Cement composition

Main purpose of our experimental study was to determine the influences of *ground granulated blastfurnace slag (GGBS) content of cements on post-heating characteristics* of hardened cement paste as well as that of concrete. The following cements were involved in the comparative study: Portland cements: CEM I 52,5 N, CEM I 42,5 N; Portland-slag cements: CEM II/A-S 42,5 N, CEM II/B-S 32,5 R; and Blastfurnace cements: CEM III/A 32,5 N, CEM III/B 32,5 N-S.

Clinker to slag proportions of cements tested in addition to their detailed chemical compositions. Data are given in Tables 1 and 2, respectively. The slag contents were 0, 16, 25, 41 or 66 m% within the total mass of cements. All of the tested cements were produced by the same cement plant (Duna-Dráva Cement, Heidelberg Cement Group) in order to have the same type of clinker and slag.

Cement clinkers and slag were ground together during the production of cement.

2.2 Test specimens and variables

Tests on hardened cement paste specimens (cubes of 40 mm sides)

The test variables were type of cements (Tables 1 and 2) and maximum temperatures (Table 3); the test constants were water to cement ratio ($w/c=0.43$) and cement content, while the studied characteristics were surface cracking (macroscopic observation), compressive strength and thermoanalytic characteristics.

Tests on concrete specimens (cubes of 150 mm sides)

The test variables were type of cement (Tables 1 and 2) and maximum temperatures (Table 3), the test constants were water to cement ratio ($w/c=0.43$), cement content as well as type and grading of aggregate (Table 4), while the studied characteristics were surface cracking, compressive strength and microscopic observation of morphology scanning electron microscope images.

The parameter combinations resulted in altogether 340 specimens including five measurements to every combination of parameters (Table 3).

2.3 Test methods

Casted specimens were removed after 24 hours from the formwork, then specimens were stored in water for 7 days and kept at laboratory conditions (temperature 20 °C , 65% relative humidity) until testing in accordance with the standard [28]. The specimens were 30 days old at the date of testing.

Our experimentally applied heating curve was similar to the standard fire curve (in accordance with EN 1991.1.2 [4]) up to 800 °C. Specimens were kept for two hours at the various maximum temperature levels (Fig. 1). Specimens were then slowly cooled down (Fig 1) in laboratory conditions for further observations. The heating process (temperatures, heating rate, cooling rate) are given on Fig 1. During our experiment electric furnace was used. The heating process was direct program controlled. The compressive strength was measured on the cooled down specimens and the average values of the measurements were analysed.

Changes in phases were followed by thermoanalytical methods (TG/DTG/DTA) using Derivatograph-Q 1500 D. This equipment is able to collect TG/DTG/DTA data from the same measurement simultaneously. For computational evaluation of the thermoanalytical test results Winder (Version 4.4.) software was used. There is a simultaneous procedure where the TG (Thermogravimetry) and DTA (Differential Thermal Analysis) thermoanalytical methods can be combined. As the result of thermogravimetry (TG) the first derivative of thermogravimetric curve (DTG) is also obtained. Reference material was alumina (Al_2O_3), and $10^\circ Cmin^{-1}$

heating rate was chosen up to ~1000 °C. Tests were carried out in air atmosphere. Part of the specimens was ground in an agate mortar making powder form sample. Mass of sample was ~300 mg. The test results were evaluated by using Winder V 4.4 software.

To study the morphology of the samples SEM images were obtained by a JEOL JSM-5500LV scanning electron microscope. For the observation the specimens were freshly split avoiding the surface from the carbonation and to reach the appropriate size of the sample. Further preparation was coating of the sample's surface made in vacuum with evaporation of gold/palladium (Au/Pd). Acceleration voltage of 20 kV was used. Samples were imaged under high vacuum conditions. Actual magnifications are printed on the SEM pictures.

3. Results and discussions

Results on surface cracking and residual compressive strength after exposing to high temperatures are presented and discussed herein.

3.1 Development of surface cracks

3.1.1 Hardened cement paste specimens

Temperature loading on hardened cement paste specimens caused chemical and physical changes leading to surface cracking. Development of surface cracks as a result of the elevated temperatures is presented in Fig. 2.

In the case of Portland cement specimens (CEM I 52,5 N, CEM I 42,5 N) cracks already formed by heating up to 500 °C, and the size and number of cracks considerably increased by heating up to 800 °C (see 1st column of Fig. 2). Crack development is explained by the chemical reactions in the hardened cement paste, i.e. dehydration of portlandite, $\text{Ca}(\text{OH})_2$ at about 450 °C and decomposition of CSH at about 750 °C.

In the case of Portland-slag cement specimens (CEM II/A-S 42,5 N; CEM II/B-S 32,5 R) only small cracks appeared by heating up to 500 °C, and the amount and size of cracks increased in the case of specimens heating up to 800 °C (see 2nd column of Fig. 2). With the increasing substitution of cement with slag the production of portlandite in the hardened cement paste decreases; thus, less portlandite dehydrates at about 450 °C, which may give the explanation of decreased amount of cracks.

By Blastfurnace cement specimens (CEM III/A 32,5 N; CEM III/B 32,5 N-S) in the case of CEM III/A 32,5 N there were only few small cracks by heating up to 500 °C (see 3rd column of Fig. 2), while by using CEM III/B 32,5 N-S we did not observe any surface cracks heating either up to 500 °C or to 800 °C (see 4th column of Fig.

2). Explanation: amount of surface cracks can be related to the fact that these cements contain the highest amount of slag.

The higher the replacement of the clinker by GGBS (ground granulated blastfurnace slag) in the cements, the lower the amount of Ca(OH)_2 formed due to the hydration. Additionally the amount of Ca(OH)_2 decreases with the pozzolanic reaction between GGBS and Ca(OH)_2 , too. Development of cracking after heating is related to rehydration of CaO resulting 44% volume increase [24]. CaO is the product of dehydrated Ca(OH)_2 . Development of cracking followed after cooling down (kept the specimens in laboratory conditions). Number of cracks increased as a function of time after cooling down.

3.1.2 Hardened concrete specimens

High temperatures may induce changes both in the hardened cement paste and in the aggregates of concrete. Change in crystal structure of quartz aggregates causes 5.7% expansion at about 573 °C [25]. There is an important question of whether the observations on hardened cement paste specimens (discussed in Chapter 3.1.1) are also valid for concrete specimens, or there is any additional influence due to the above mentioned expansion of aggregates at high temperatures. In Fig. 3 the development of surface cracks in concrete specimens after high temperature (800 °C) loading is presented. Comparison of the 1st column (left hand side) of Fig. 2 (800 °C) to the 1st column (left hand side) of Fig. 3 indicates more dispersed crack pattern for concrete (Fig. 3) related to hardened cement paste (Fig. 2) which may show the advantageous influence of aggregates in distributing cracks. With the increasing slag content of cement, the size and number of surface cracks were also decreased in concrete specimens (Fig. 3) similar to the hardened cement paste specimens (compare 1st and 2nd left hand side columns of Fig. 3).

3.2 Compressive strength

In this chapter compressive strength measurements of hardened cement paste and concrete specimens are presented and discussed.

3.2.1 Hardened cement paste

In Fig. 4 the compressive strengths of the hardened cement paste specimens are presented related to the compressive strength measured at 20 °C ($f_{c,T}/f_{c,20}$ called residual relative compressive strength) as functions of the maximum temperature and the cement type.

The relative residual compressive strength decreases up to 150 °C heat loading, then increases up to 300 °C. In the case of higher temperatures than 300 °C the residual relative compressive strength decreases again. Specimens loaded up to 300 °C show higher residual strength comparing with the average strengths measured on specimens loaded up to 150 °C because the intensive dehydration in the temperature interval between 60 and 180 °C probably causes the hydration of the unhydrated cement grains in the microstructure. This was proved by the thermoanalytical measurements. In the case of Portland cement specimens (CEM I 42,5 N) the average of residual relative compressive strength of the test specimens was 35% heating up 500 °C and further 10 % by heating up to 800 °C. For Portland-slag cement specimens (CEM II/A-S 42,5 N; CEM II/B-S 32,5 R) the average of the residual relative strength was 41 % and 47 % by heating up to 500 °C and further 17 % and 20 % by heating up to 800 °C, respectively. While in the case of Blast furnace cement specimens (CEM III/A 32,5 N; CEM III/B 32,5 N-S) the average of the residual relative strength was 59 % and 65 % by heating up to 500 °C and further 37 % and 44 % by heating up to 800 °C, respectively.

To sum up these results, the temperature load at 800 °C caused increasing residual relative compressive strength with the increase of slag content. The most considerable difference was observed between Portland cement (CEM I 52,5 N, slag content: 0 %) and Blast furnace cement (CEM III/B 32,5 N-S, slag content: 75 %). The results of the compressive strength tests are in accordance with the crack developments. The most significant cracks appeared on test specimens made of Portland cement, and the compressive strength loss was also the highest.

3.2.2 Concretes

Compressive strength measurements on concrete specimens made with quartz gravel aggregates and different types of cements are presented in Fig. 5 as a function of the maximal value of temperature load. The following conclusions can be drawn:

- The relative residual compressive strength decreases up to 150 °C heat loading, then increases up to 300 °C. In the case of higher temperatures than 300 °C the residual compressive strength decreases again.
- Concretes made of cements CEM II/A-S 42,5 N, CEM III/A 32,5 N and CEM III/B 32,5 N-S have higher residual relative compressive strength than concrete made of Portland cement CEM I 42,5 N.

- With increasing the slag content of cement the relative residual compressive strength of concrete improves.
- After 800 °C temperature loading, the relative residual compressive strength of concrete made of CEM I 52,5 N and CEM III/B 32,5 N was 23 % and 44 %, respectively, resulting approximately double value as for Portland cement counting specimens.

Our conclusion is that after temperature load the relative residual compressive strength of concrete is significantly increased if cements contain high amounts of slag.

3.3 Scanning electron microscopy observations

Differences both in surface cracking and in compressive strength can be explained by the different microstructure of the concrete using Portland cement or slag Portland cement. Different microstructures of concretes using Portland cement or slag containing cements are shown in Figs. 6 and 7 taken by scanning electron microscopy. In the case of concrete made with Portland cement large portlandite plates ($\text{Ca}(\text{OH})_2$) can be seen on the surface of quartz aggregates. Smaller crystals on the surface of portlandite indicate CSH phases (Fig. 6). In the case of concrete made with Portland-slag cement large plates of portlandite were not observed. Observations were proved by the similar SEM analyses made on cement pastes by Kopecskó [29].

3.4. Thermal analysis (TG/DTG/DTA)

Thermal analyses were made on freshly ground powder samples of hardened cement paste specimens. Derivative thermogravimetric (DTG) curves were selected to represent the comparative results. DTG curves are shown in Fig. 8. Significant peaks indicate the loss of absorptive water and the dehydration of AFt and/or AFm phases (e.g. ettringite and/or monosulphate) as well as the dehydration of portlandite ($\text{Ca}(\text{OH})_2$, with about 450 °C peak temperature) as a function of increasing temperature.

Different amounts of portlandite formed by the cement hydration supported the results of the compressive strength measurements. Except of ordinary Portland cement in the heterogeneous cements different amount of the cement clinkers are substituted by the supplementary cementing materials (in our case with GGBS). The clinker to slag ratios in cements determine the amount of portlandite because this compound is the product of the hydration of calcium-silicate clinker minerals (C_3S and C_2S). In slag cements less calcium-silicates are present; therefore, the amount of the hydration product, portlandite is lower. In addition to the above mentioned causes portlandite contributes to GGBS hydration due to pozzolanic reaction in formation of calcium-silicate hydrates (CSH-s). In this reaction slag consumes portlandite, so the amount of portlandite is decreasing during the GGBS

hydration, too. The decreasing thermogravimetric mass loss (TG) of portlandite in the case of increasing slag contents in cements are in accordance with the results of relative residual compressive strengths. As a result of heat load higher than 450 °C the portlandite phase in the specimens dehydrates. The product of this dehydration process is calcium-oxid (CaO) which in the humid laboratory condition during cooling and storing easily rehydrate. Intensive crack development was observed on the surface of the already cooled down specimens. The cement paste specimens were made without adding any aggregate (e.g. sand), so the crack development is not connecting with the phase transition of quartz.

4. Conclusions

The purpose of the present study was to analyse the post-heating characteristics of hardened cement paste and that of hardened concrete. Main experimental parameters were the cement types (6 different types: Portland cements, slag Portland cements and slag cements) and the maximal temperature of heat treatment up to 800 °C (20 °C, 50 °C, 150 °C, 300 °C, 400 °C, 500 °C, 600 °C, 800 °C), respectively.

Water to cement ratio was kept constant ($w/c=0.43$). The same consistency was reached by using superplasticizer. Grading curve (particle size distribution) of aggregates was the same for all of the concrete specimens.

Present studies included analysis of surface cracking, compressive strength and thermal analyses (TG/DTG), and scanning electron-microscopic observations (SEM).

From our results the following conclusions can be drawn:

1. Slag content of cement has an important influence on post-heating characteristics of concrete.
2. Relative post-heating compressive strength increases with increasing slag content of cement.
3. Amount of surface cracking (sum of lengths and widths) is reduced by the increasing slag content of cements.
4. Thermogravimetric investigations indicated decreasing mass loss between 400 °C to 600 °C by increasing slag content of cement. This observation supports Conclusion 2.

Above conclusions were obtained on small cement specimens (cubes of 40 mm) and on concrete specimens (cubes of 150 mm sides).

Acknowledgements

The authors express their acknowledgements to the Duna-Dráva Cement Heidelbergcement Group for the financial support of the experimental study. Report number: 34489-003-EA. I. M. S. thanks for a János Bolyai Research Fellowship of the Hungarian Academy of Sciences and an OTKA-PD-109129 grant.

References

- [1] Schneider U. Concrete at high temperatures - a general review. *Fire Safety Journal*, 1988;13:55-68.
- [2] Kordina K. Fire resistance of reinforced concrete beams. (Über das Brandverhalten punktgeschützter Stahlbetonbalken), Deutscher Ausschuss für Stahlbeton, Heft 479, ISSN 0171-7197, Beuth Verlag GmbH, Berlin, 1997.
- [3] Waubke NV. Physicalise analysis of strength reduction of concrete up to 1000 °C. (Über einen physikalischen Gesichtspunkt der Festigkeitsverluste von Portlandzement-betonen bei Temperaturen bis 1000 °C-Brandverhalten von Bauteilen), Dissertation, TU Braunschweig, 1973.
- [4] Eurocode 1. Basis of design and actions on concrete structures. Part 2-2: Actions on structures exposed to fire, EN 1991-1-2:2002, November 2002.
- [5] American Concrete Institute. ACI/TMS 216 Standard Method for Determining Fire Resistance of Concrete and Masonry Construction Assemblies. Framington Hills, MI, 1997.
- [6] Ministry of Construction. Ed.. Taika Seinou Kenshouhou no Kaisetu Oyobi Keisanrei tosonso Kaisetu. Guidline on Vertification Method for Fire Resistance and Exemplares. Inoue Shoin, 2001.
- [7] Khoury GA, et al. Fire Design of Concrete Materials Structures and Modelling. 1st fib Congress, Osaka, Japan, Oct. 2001.
- [8] Khoury GA. Effect of heat on concrete material. Imperial College report. 1995, pp. 73.
- [9] Khoury GA, Grainger BN, Sullivan PJE. Transient thermal strain of concrete: literature review, conditions within specimen and behaviour of individual constituents. *Magazine of Concrete Research*. 1995;37:48-56.
- [10] Budelman H. Strength of concrete with different moisture content after elevated temperature. (Zum Einfluss erhöhter Temperatur auf Festigkeit und Verformung von Beton mit unterschiedlichen Feuchtegehalten), Heft 76, ISBN 3-89288-016-6, Braunschweig, 1987.
- [11] Schneider U, Lebeda C. Fire protection of builldings. (Baulicher Brandschutz). ISBN 3-17-015266-1, W. Kohlhammer GmbH., Stuttgart, 2000.

- [12] Schneider U. Properties of Materials at High Temperatures, Concrete. RILEM Publ., 2nd Edition, Gesamthochschule Kassel, Universität Kassel, 1986.
- [13] *fib* bulletin 38, Fire design of concrete structures- materials,, structures and modelling. ISBN: 978-2-88394-078-9, 2007.
- [14] Barbara P, Iwona W. Comparative investigations of influence of chemical admixtures on pozzolanic and hydraulic activities of fly ash with the use of thermal analysis and infrared spectroscopy. *Journal of Thermal Analysis and Calorimetry*. 2015; 120 119-127.
- [15] Yun L, Hung-Liang C. Thermal analysis and adiabatic calorimetry for early-age concrete members. *Journal of Thermal Analysis and Calorimetry*. 2015;122:937-945.
- [16] Grainger BN. Concrete at High Tempereatures. Central Electricity Resarch Laboratories, UK, 1980.
- [17] Dias WPS, Khoury GA, Sulivan PJE. Mechanical properties of hardened cement paste exposed to temperatures up to 700 °C. *ACI Materials Journal*. 1990;87:160-166.
- [18] Xu Y, Wong YL, Poon CS, Anson M. Impact of high temperature on PFA concrete. *Cement and Concrete Research*. 2001;31:1065-1073.
- [19] Khoury GA, Sarshar R, Sulivan PJE. Factors affecting the compressive strength of unsealed cement paste and concrete at elevated temperatures up to 600 °C. *Proc. 2nd Int. Workshop on Mechanical Behaviour of Concrete under Extreme Thermal and Hygral Conditions*. ISSN 0863-0720, pp. 89-92, Weimar, 1990.
- [20] Khoury GA, Grainger BN, Sullivan PJE. Transient thermal strain of concrete: literature review. conditions within specimen and behaviour of individual constituents. *Magazine of Concrete Research*. 1985;37:37-48.
- [21] Schneider U, Weiß R. Kinethical treatment of thermal deterioration of concretes and its mechanical influences. *Cement and Concrete Research*. 1997;11:22-29
- [22] Bazant PZ, Kaplan FM. Concrete at High Temperetures. Longman Group Limited. London, ISBN: 0-582-08626-4, 1996.
- [23] Hinrichsmeyer K. Analysis and Modeling of Concrete Subjected to High Temperature. (Strukturorientierte Analyse und Modellbeschreibung der thermischen Schädigung von Beton) Heft 74 IBMB, Braunschweig, 1987.
- [24] Eurocode 2. Design of concrete structures. Part 1 General rules - Sructural fire design EN 1992-1-2:2002, February 25.
- [25] Thielen KCh. Strength and Deformation of Concrete Subjected to high Temperature and Biaxial Stress - Test and Modeling, (Festigkeit und Verformung von Beton bei hoher Temperatur und biaxialer

- Beanspruchung – Versuche und Modellbildung), Deutscher Ausschuss für Stahlbeton, Heft 437, ISSN 0171-7197, Beuth Verlag GmbH. Berlin, 1994.
- [26] Hoj NH. Fire Design of Concrete Structures. Proceedings of fib Symposium on Keep concrete attractive, edited by Gy. L. Balázs. A. Borosnyói, 23-25 May 2005 Budapest. pp.: 1097-1105, 2005.
- [27] Gambarova PG. Opening Adresses on Some Key Issues Concerning R/C Fire Design. Proceedings for Fire Design of Concrete Structures: What now?, What next?, edited by: P.G., Gambarova. R., Felicetti. A., Meda. P., Riva, December 2-3, 2004.
- [28] MSZ EN 196-2:2013 Methods of testing cement, Chemical analysis of cement.
- [29] Kopecskó K. Chloride ion binding capacity of clinker minerals and cements influenced by steam curing. PhD Thesis, 2006. Budapest, http://www2.epito.bme.hu/eat/phdk/Kopecsko_Katalin_PhD.pdf

Tables

Table 1 Clinker and slag contents of tested cements (data by Duna-Dráva Cement Heidelbergcement Group)

| | CEM I 52,5 N | CEM I 42,5 N | CEM II/A-S 42,5 N | CEM II/B-S 32,5 R | CEM III/A 32,5 N | CEM III/B 32,5 N-S |
|------------------|-----------------|-----------------|----------------------|----------------------|---------------------|-----------------------|
| clinker | 95.0 | 95.0 | 76.3 | 72.4 | 50.6 | 26.8 |
| slag | 0.0 | 0.0 | 16.0 | 24.6 | 41.1 | 66.0 |
| limestone | 0.0 | 0.0 | 2.7 | 3.0 | 3.2 | 2.2 |
| gypsum | 5.0 | 5.0 | 5.0 | 5.0 | 5.0 | 5.0 |

Note: Cement clinker and slag were ground together during production of cement

Table 2 Chemical composition of tested cements (m%) (data by Duna-Dráva Cement Heidelbergcement Group)

| Comp. | CEM I 52,5 N | CEM I 42,5 N | CEM II/A-S 42,5 N | CEM II/B-S 32,5 R | CEM III/A 32,5 N | CEM III/B 32,5 N-S |
|------------------------------------|-----------------|-----------------|----------------------|----------------------|---------------------|-----------------------|
| SiO₂ | 20.59 | 19.84 | 22.77 | 23.9 | 27.19 | 31.39 |
| Al₂O₃ | 5.55 | 5.38 | 5.83 | 5.92 | 6.46 | 7.28 |
| Fe₂O₃ | 3.21 | 3.22 | 2.97 | 2.55 | 2.63 | 2.51 |
| CaO | 65.02 | 64.90 | 60.30 | 55.33 | 52.80 | 46.28 |
| MgO | 1.44 | 1.38 | 2.51 | 4.15 | 4.30 | 5.93 |
| SO₃ | 2.88 | 2.97 | 3.00 | 3.02 | 3.04 | 3.01 |
| K₂O | 0.78 | 0.78 | 0.80 | 0.5 | 0.78 | 0.83 |
| Cl | 0.0055 | 0.0048 | 0.0056 | 0.0016 | 0.0048 | 0.002 |

Table 3 Test parameters

| Max. Temp. / °C | CEM I 52,5 N | CEM I 42,5 N | CEM II/A-S 42,5 N | CEM II/B-S 32,5 R | CEM III/A 32,5 N | CEM III/B 32,5 N-S |
|-----------------------|-----------------|-----------------|----------------------|----------------------|---------------------|-----------------------|
| 20 | P | P, C | P, C | P | P, C | P, C |
| 50 | P | P, C | P, C | P | P, C | P, C |
| 150 | P | P, C | P, C | P | P, C | P, C |
| 300 | P | P, C | P, C | P | P, C | P, C |
| 400 | - | C | C | - | C | C |
| 500 | - | C | C | - | C | C |
| 600 | P | P, C | P, C | P | P, C | P, C |
| 800 | P | P, C | P, C | P | P, C | P, C |

Remark: 5 specimens were tested to every parameter, combination

P: hydrated cement paste specimens (36*5=180 specimens);

C: concrete specimens (32*5=160 specimens)

Table 4: Composition of tested concrete mixes amount of composites/ kgm^{-3}

| Cement type | CEM I 52,5 N | CEM II/A- S 42,5 N | CEM III/A 32,5 N | CEM III/B 32,5 N-S |
|-------------------------|-----------------|-----------------------|---------------------|-----------------------|
| cement | 350 | 350 | 350 | 350 |
| water | 151 | 151 | 151 | 151 |
| river sand 0-4 mm | 912 | 912 | 912 | 912 |
| river gravel 4-8 mm | 485 | 485 | 485 | 485 |
| river gravel 8-16 mm | 544 | 544 | 544 | 544 |
| Super plasticizer | 1.4 | 1.5 | 1.7 | 1.8 |

Figures

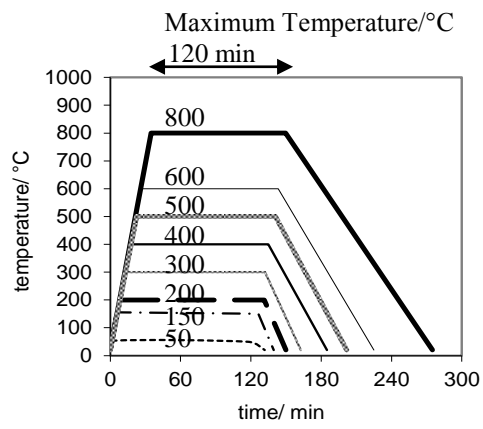


Fig. 1 Schematic representation of heating curves

| Hardened cement paste specimens with | | | | Max. temp. /°C |
|--|-------------------|------------------|--------------------|----------------|
| CEM I 52,5 N | CEM II/A-S 42,5 N | CEM III/A 32,5 N | CEM III/B 32,5 N-S | |
| a | | | | 500 |
| b | | | | 800 |
| Crack maps separated from above pictures | | | | |
| A | | | | 500 |
| B | | | | 800 |
| 40 mm | | | | |

Fig. 2 Effect of cement type on the development of surface cracks as a result of the elevated temperature (hardened cement paste specimens, w/c=0.43)

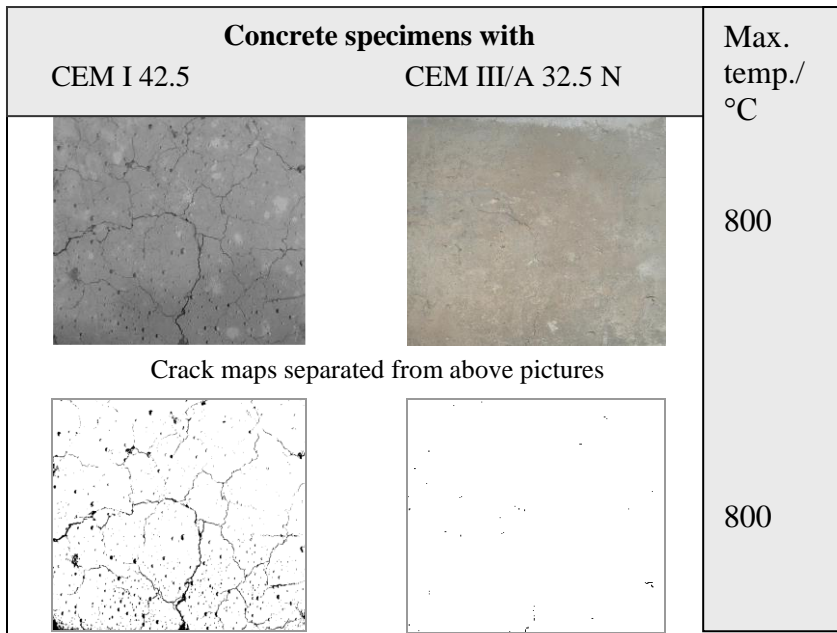


Fig. 3 Effect of cement type on the development of surface cracks as a result of the elevated temperature (concrete specimens, w/c=0.43)

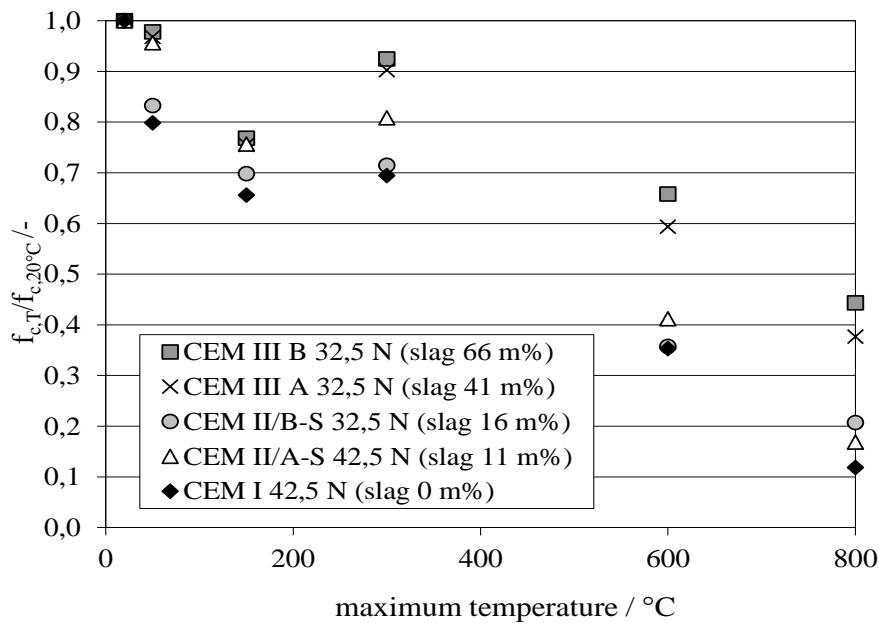


Fig. 4 Residual compressive strength of hardened cement paste with different cement types (strength values are related to strength values of 20°C); Reference values (Nmm⁻²): CEM I 42,5 N, 103.1; CEM II/A-S, 98.5; CEM II/B-S, 82.5; CEM III/A-S, 75.1; CEM III/B-S, 63.8)

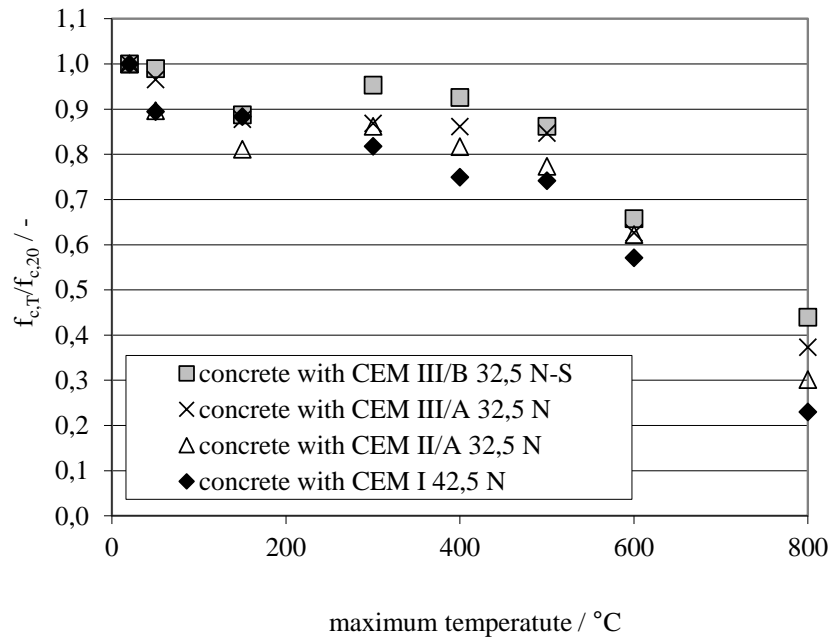


Fig. 5 Residual compressive strength of concrete as functions of temperature and type of cement (all values are calculated from three measurements, the average values are represented), Reference values (Nmm^{-2}): CEM I 42,5 N, 64.3; CEM II/A-S, 31.6; CEM II/B-S, 30.6; CEM III/B-S, 29.9)

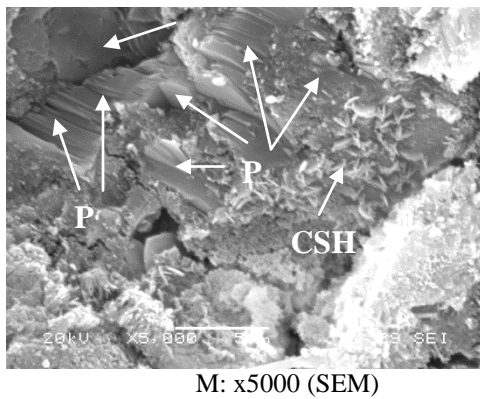
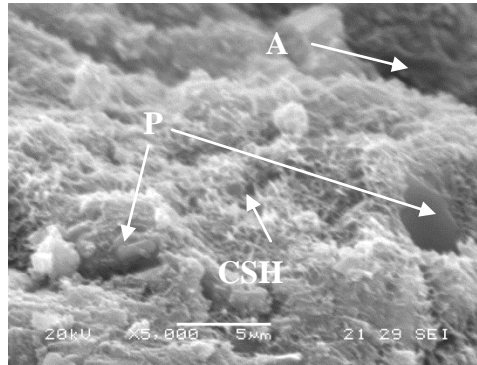


Fig. 6 Concrete using Portland cement Notation: **A** - aggregate (quartz gravel), **P** – portlandite, **CSH** - calcium-silicat-hydrate



M: x5000 (SEM)

Fig. 7 Concrete using Blast furnace cement Notation: **A** - aggregate (quartz gravel), **P** – portlandite, **CSH** - calcium-silicat-hydrate

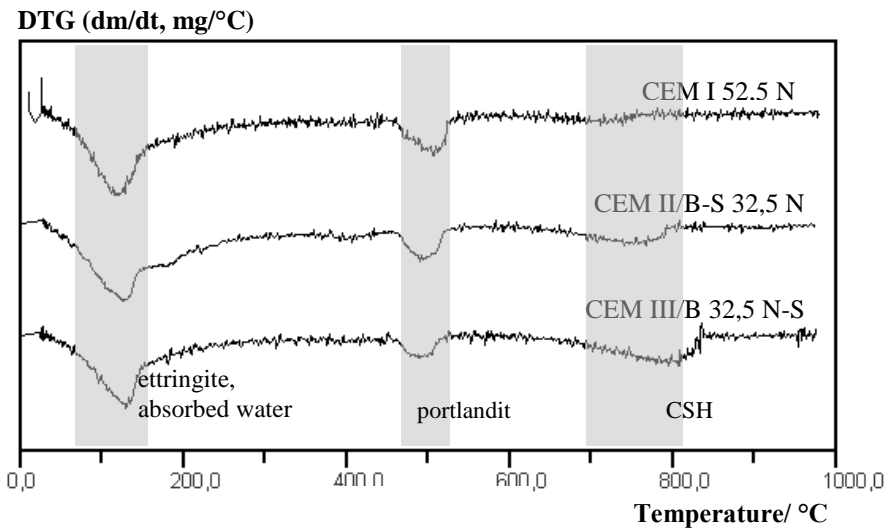
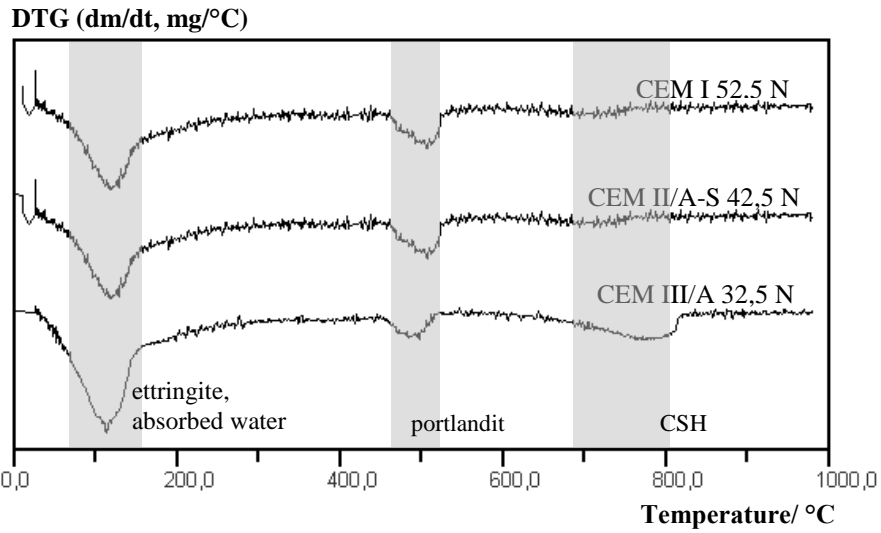


Fig. 8 Results of thermoanalytic measurement: the 1st derivatives of thermogravimetric mass loss (DTGs) in case of CEM I 52,5 N, CEM II/B-S 32,5 N and CEM III/B 32,5 N-S